Current Biology, Volume *31*

Supplemental Information

Thalamic input to motor cortex facilitates goal-directed action initiation

Naoya Takahashi, Sara Moberg, Timothy A. Zolnik, Julien Catanese, Robert N.S. Sachdev, Matthew E. Larkum, and Dieter Jaeger

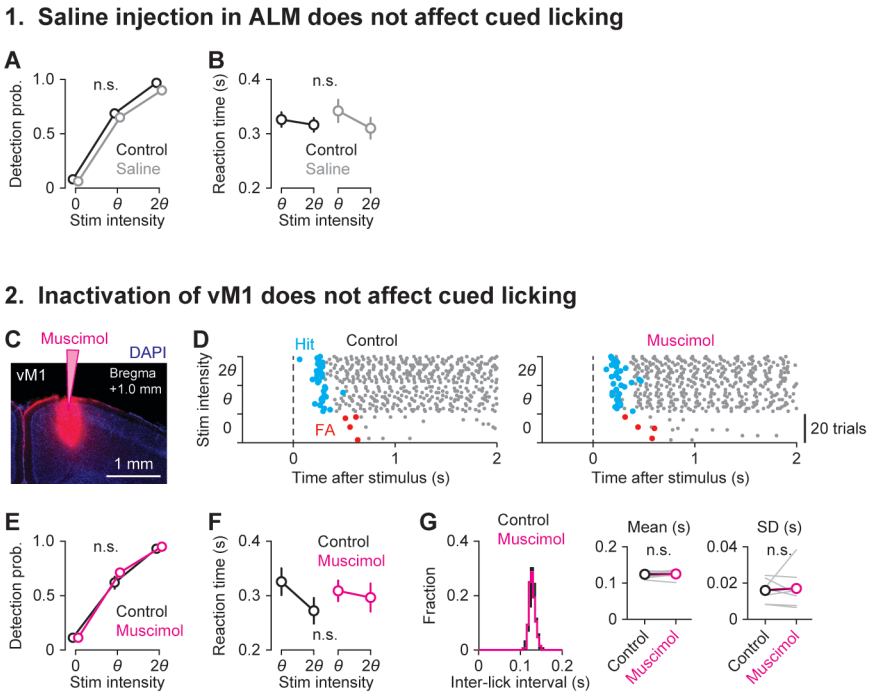

Figure S1. Impact of vM1 inactivation on cued licking. Related to Figure 1.

(A, B) Behavioral comparisons before (black) and after (gray) saline injection in the left ALM. (A) Detection probability (n = 8 sessions from 4 mice, mean ± SEM; P = 0.10, two-way repeated-measure ANOVA). (B) Reaction times for threshold and salient stimuli (n = 8 sessions from 4 mice, mean ± SEM; P = 0.81, two-way repeated-measure ANOVA).

(C) Site and diffusion of unilateral muscimol injection in the left vM1.

(D) Raster plot showing lick responses (gray dots) throughout a representative behavioral session before (left) and after (right) muscimol injection.

(E–G) Behavioral comparisons before (black) and after (magenta) muscimol injection. (E) Detection probability (n = 8 sessions from 4 mice, mean ± SEM; P = 0.20, two-way repeated-measure ANOVA). (F) Reaction times for threshold and salient stimuli (n = 8 sessions from 4 mice, mean ± SEM; P = 0.86, two-way repeated-measure ANOVA). (G) Histograms of inter-lick intervals in an example session (left). Insets: means (middle) and SDs (right) of inter-lick intervals (n = 8 sessions from 4 mice; P = 0.60 for means, P = 0.74 for SDs, paired t-test).

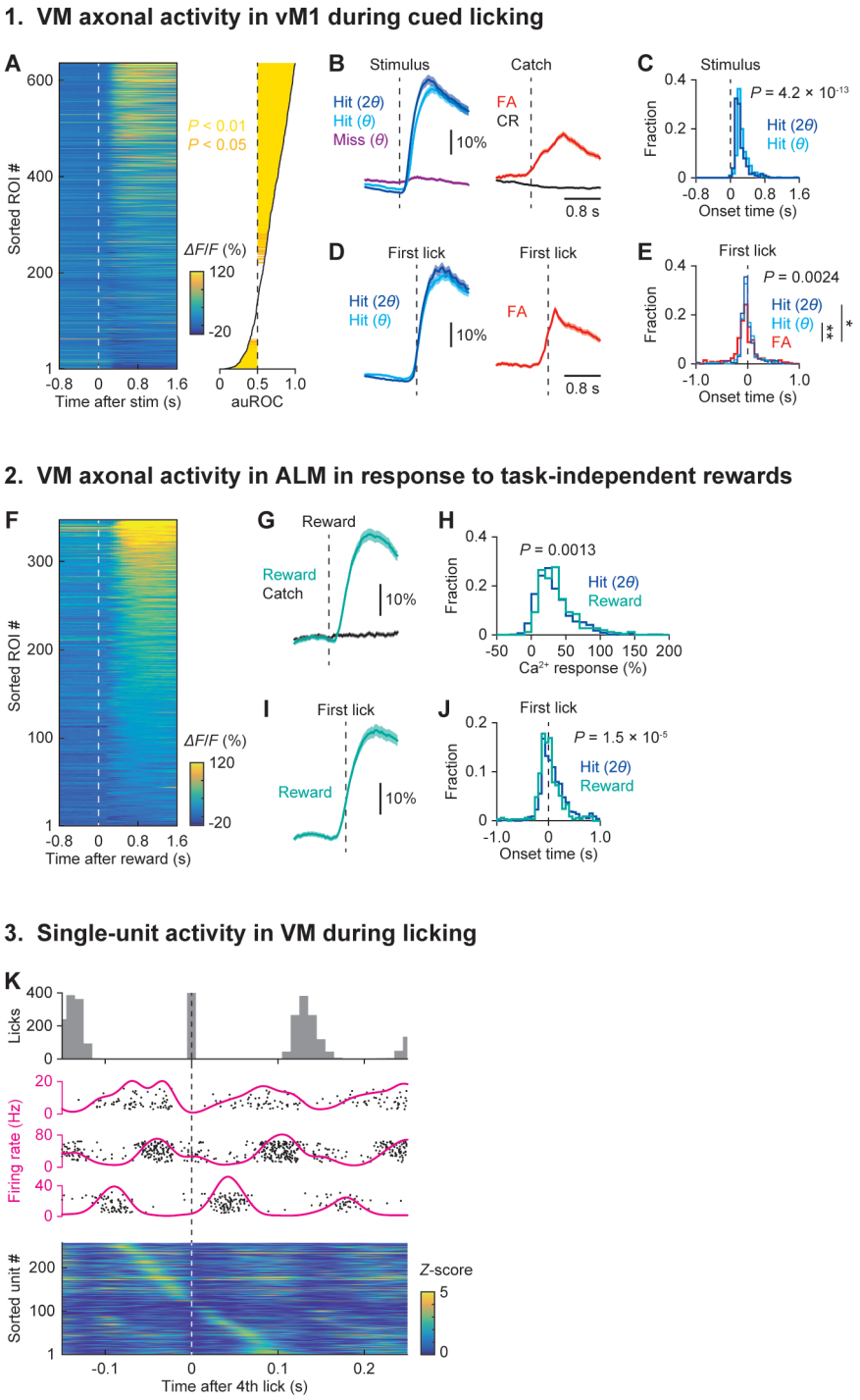

Figure S2. VM axonal activity and VM single-unit activity during licking. Related to Figure 2.

(A) Left: Ca^{2+} activity of VM axonal boutons in vM1 averaged across hit trials in response to threshold whisker stimuli. Right: auROCs with statistical significance indicated in colors.

(B) Left: Ca^{2+} responses to salient stimuli and threshold stimuli in hit trials (blue) vs. threshold stimuli in miss trials (purple) for axonal boutons with *auROC > 0.5 (n = 404 boutons, mean ± SEM). Right: Ca^{2+} activity associated with false alarm (red) vs. correct rejection (black) in catch trials.

(C) Histogram of onset timings of Ca^{2+} responses in hit trials (n = 404 boutons; Wilcoxon singed-rank test).

(D) Ca^{2+} responses of axonal boutons with *auROC > 0.5 aligned by the timing of the first lick in hit (left) and false alarm trials (right) (n = 404 boutons, mean ± SEM).

(E) Histogram of onset timings of Ca^{2+} responses aligned by the first lick in hit and false alarm trials (n = 404 boutons for hit trials and 352 boutons for false alarm trials; Kruskal-Wallis test with Scheffe's post hoc comparisons, *P = 0.025, **P = 4.7×10^{-3}).

(F) Ca^{2+} signals in VM axonal boutons in ALM averaged across trials in response to randomly delivered water rewards (n = 331 boutons from 4 sessions from 2 mice), sorted according to the peak amplitude.

(G) Ca^{2+} responses to random rewards (n = 331 boutons, mean ± SEM) compared with those in catch (no reward) trials.

(H) Histogram of amplitudes of Ca^{2+} responses to random rewards compared with those to salient stimuli in hit trials during the cued licking task (n = 331 boutons for random reward trials and 856 boutons for hit trials; Mann-Whitney U test).

(I) Ca^{2+} responses to random rewards, aligned by the timing of the animal's first lick (n = 331 boutons, mean ± SEM).

(J) Histogram of onset timings of Ca^{2+} responses aligned by the first lick in random reward and hit trials (n = 331 boutons for random reward trials and 856 boutons for hit trials; Mann-Whitney U test).

(K) Single-unit recording from the left VM during contralateral licking. Top: Histogram of lick times aligned by the 4th lick in a lick train triggered by reward availability (bin = 10 ms, n = 1190 trials). Middle: Raster plots of single-unit activity of three representative VM neurons (black) around the 4th lick, overlaid with firing rates averaged across trials (smoothed with a 10-ms Gaussian kernel; magenta). Bottom: Normalized spike density functions of single-unit activity of VM neurons that were significantly modulated during licking (n = 258 neurons with a peak Z score > 1.96).

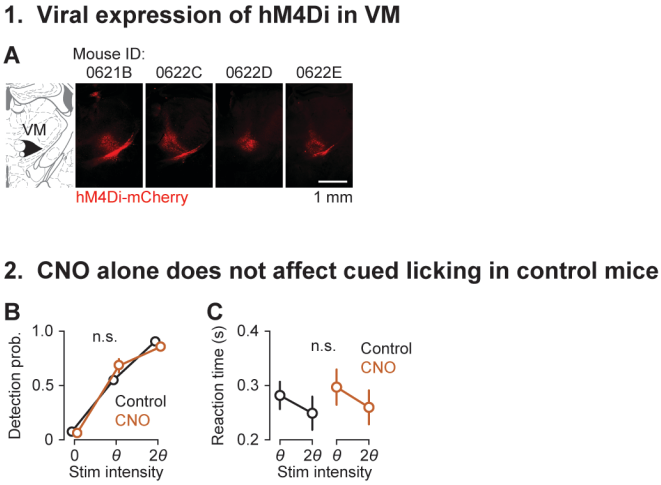

Figure S3. hM4Di expression in virally transduced mice and impact of CNO on behavior in control mice. Related to Figure 3.

(A) Fluorescent images of AAV-hM4Di-mCherry injection sites in the left VM thalamus.

(B, C) Behavioral comparisons before (black) and after (brown) CNO injection in left ALM of control mice (not expressing hM4Di). (B) Detection probability (n = 8 sessions from 4 mice, mean ± SEM; P = 0.20, two-way repeated-measure ANOVA). (C) Reaction times for threshold and salient stimuli (n = 8 sessions from 4 mice, mean ± SEM; P = 0.13, two-way repeated-measure ANOVA).

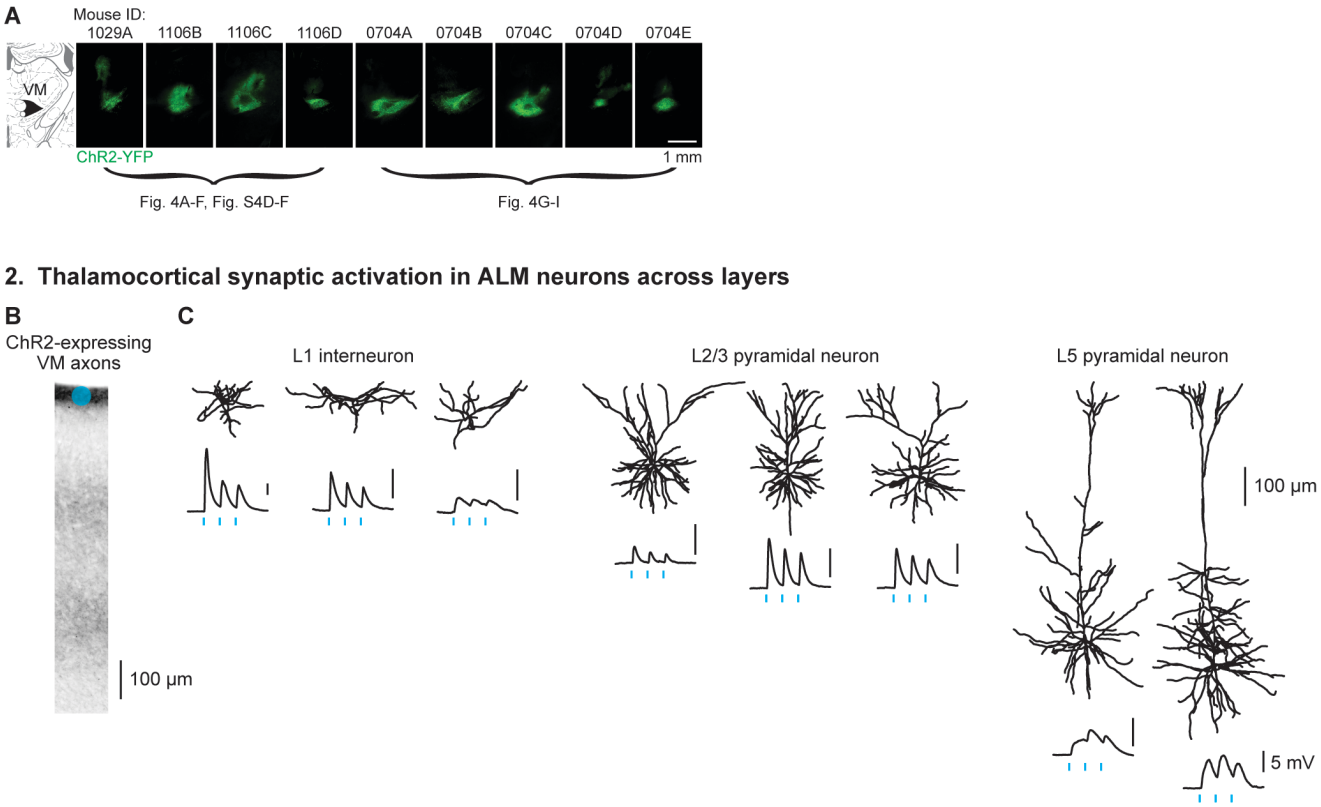

Figure S4. Impact of photostimulation of VM axons on ALM neurons and mouse behavior. Related to Figure 4.

(A) Fluorescent images of AAV-ChR2-YFP injection sites in the left VM thalamus.

(B) ChR2-expressing VM axonal fibers (black) in ALM. The blue circle indicates the photostimulation site.

(C) Top: Reconstructed morphologies of 8 ALM neurons in L1, L2/3, and L5. Bottom: EPSPs responses to photostimulation in L1 (3 pulses at 20 Hz; indicated by blue lines).

(D–F) Impact of photostimulation on psychometric parameters, i.e., (D) false alarm rate, (E) gain (slope), and (F) threshold intensity (P = 0.61) (n = 16 sessions from 4 mice, Wilcoxon signed-rank test).